Transactions of the Materials Research Society of Japan 29 [2] 413-416 (2004)

The Effect of Processing Temperature on the Columnar Structure of ZrO_2-4mol%Y_2O_3 Thermal Barrier Coatings Fabricated by Electron Beam Physical Vapor Deposition

Kunihiko Wada, Norio Yamaguchi and Hideaki Matsubara
Materials Research and Development Laboratory, Japan Fine Ceramics Center
2-4-1 Mutsuno, Atsuta-ku, Nagoya 456-8587, JAPAN
Fax: 81-52-871-3599, e-mail: wada@jfcc.or.jp

Textures of ZrO_2-4mol%Y_2O_3 layers produced by electron beam physical vapor deposition in the temperature range from 1223 K to 1303 K were investigated. The processing temperatures have a strong influence on the growth of the columnar grains in the coating layer. As the processing temperature is raised, the widths of the columnar grains increase. The relationship between the distance from the substrate/coating interface and the mean width of the columnar grains at each processing temperature can be plotted linearly on a double logarithmic scale. The gradients were 0.52 ~ 0.58 over the temperature range and these values are consistent with an estimation based on the "competitive-crystal-growth model". The density of nuclei on the substrate at each deposition temperature was estimated by extrapolating the fitted columnar grain width–position curve. The data fitted the Arrhenius equation and thus the degree of supercooling plays an important role in the initial nucleation during EB-PVD.

Key words: Electron beam physical vapor deposition (EB-PVD), Thermal barrier coating (TBC), Gas turbine, Crystal growth

1. INTRODUCTION

Combustion gas temperatures of advanced land-based gas turbines have approached 1500 °C in recent years [1,2]. In order to protect the hot components from high temperature environments, thermal barrier coatings (TBCs) become an indispensable technology for advanced gas turbines [3]. TBCs usually consist of a Y_2O_3 stabilized ZrO_2 ceramic layer and an oxidation resistant metallic bond layer. Thermal spray processes are widely used in TBCs. Thermally sprayed TBCs provide economical advantages, although severe spallation of the surface ceramic layer due to thermal expansion mismatch between the ceramic layer and the substrate have been reported.

Electron beam physical vapor deposition (EB-PVD) TBCs are well-known for excellent resistance against thermal stress because of their unique columnar structure [4,5]. Since EB-PVD TBCs have been applied to the hot components in jet engines for over ten years, EB-PVD will be an important process for the next generation of land-based gas turbines.

Control of the processing parameters is key to improving the properties of EB-PVD TBCs. Deposition temperature, chamber pressure, substrate motion, surface roughness of the substrate etc. all affect the texture growth and the resulting texture changes drastically [6-9]. Although many researchers have studied the relationships, the formation mechanism of the columnar structure has not been clarified so far.

In our study, we focused on the effect of the processing temperatures on the coating textures. EB-PVD TBCs were produced at 1223 K ~ 1303 K and the crystallographic textures were observed. We discuss the kinetics of the nucleation and growth of the columnar grains quantitatively.

2. EXPERIMENTAL

The Ni-based superalloy "IN-738LC" was selected as the substrate material. Ingots were machined into 20×55×3-mm^3 coupons and their surfaces polished up to #1200 before deposition. TBC layers were formed with a high power EB-PVD coater (Von Ardenne Anlagentechnik Gmbh/TUBA 150). This coater consists of a series of three chambers; a loading chamber, heating chamber, and coating chamber, and the substrate is transferred throughout these chambers using a movable sample holder. During deposition, a 63 mm diameter ZrO_2-4mol%Y_2O_3 ingot was fed from the bottom of the coating chamber at a constant rate. The deposition times were decided from previous data of the deposition rate to control the coating thickness to about 220 μm. The pressures of the coating chamber were controlled at 1.0 Pa and each sample was rotated at 5 rpm throughout deposition. The individual processing parameters for each sample are shown in Table I. Since this coater does not have any external heating unit in the coating chamber, the EB power decides the processing temperature of the samples. Therefore, EB power of 45 kW, 50 kW and 55 kW corresponded to 1223 K, 1268 K and 1303 K, respectively. We should note that the volume of vapor is also changed by the EB power.

Table I Experimental Conditions for Samples

Sample	Depo. Temp.	EB-Power	Depo. Time	Thickness	Depo. Rate
1	1223 K	45 kW	2400 s	223 μm	5.58 μm/min
2	1268 K	50 kW	2040 s	227 μm	6.68 μm/min
3	1303 K	55 kW	1820 s	227 μm	7.48 μm/min

After deposition, XRD analysis of the surfaces of the samples was performed, and the surface and cross-sectional morphologies were observed by SEM. The mean width of columnar grains was measured from the cross-sectional SEM micrographs.

3. RESULTS AND DISCUSSION

3.1 Crystallographic Morphology of Columnar Grains

SEM micrographs of the top surfaces and cross-sections of EB-PVD TBC samples produced at 1223 K and 1303 K are shown in Fig.1. In both samples, the top surfaces consist of square-pyramidal shaped facets, and these surface facets consist of a pile of triangular planes. Well-aligned columnar grains were also observed in both the cross-sections. However, the mean width of the columnar grains in the sample deposited at 1303 K is wider than that in the one deposited at 1223 K. This result suggests that the processing temperatures strongly influence the columnar grain growth.

An SEM micrograph taken at the intercolumnar position with high magnification is shown in Fig.2. As seen in this picture, each columnar grain is covered with finer branched columns to produce a "feather-like structure". This structure was observed in all samples.

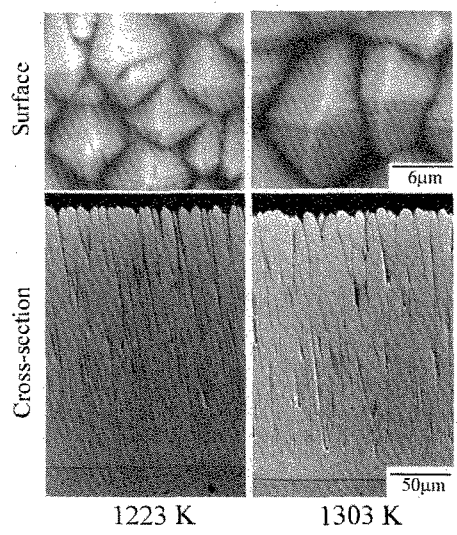

Fig.1 SEM micrographs of top surfaces and cross-sections deposited at 1223 K and 1303 K.

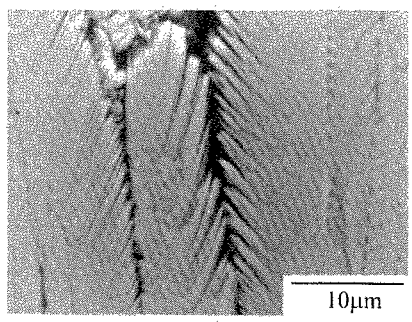

Fig.2 Feather-like structure observed in the sample deposited at 1223 K.

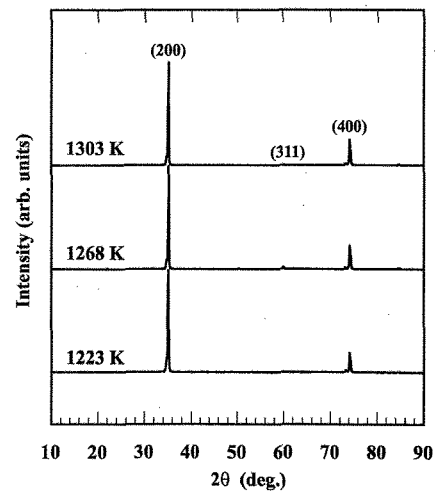

Fig.3 XRD patterns for various samples deposited at 1223 K ~ 1303 K.

There were no obvious differences between X-ray diffraction patterns for the samples fabricated at temperatures of 1223 K, 1268 K and 1303 K as seen in Fig.3. Very strong peaks of {200} and a weak (311) peak were observed. These results suggest a strong <100> orientation in the coating layer.

From these results, we can illustrate the structure of a columnar grain as in Fig.4. Most columnar grains are oriented in the <100> direction and the top surface consists of a pile of {111} facets. Many steps along the <110> direction were observed on the {111} facets. The angles between the branches in the feather-like structure and the vertical direction of the column varied from 20° to 45°. This difference is likely to be caused by the tilt of the cutting plane during sample preparation. We could not clarify the crystallographic relation between the columnar grains and the branches.

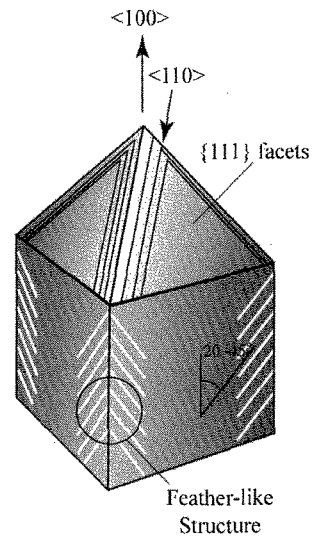

Fig.4 Schematic diagram illustrating a columnar grain in an EB-PVD TBC.

3.2 Mean width of columnar grains

The mean width of columnar grains at several positions was measured from SEM micrographs at a magnification of ×1000. The number of columnar grains that intersected with a horizontal line was counted and the mean width was obtained by dividing the length of the horizontal line by the number of columnar grains. The relationship between the mean width and the distance from the top coat/substrate interface is shown in Fig.5. As mentioned above, the width of columnar grains grows larger as the processing temperature increases. At 200 μm from the interface, the width of the columnar grains in the samples deposited at 1223 K, 1268 K and 1303 K are 4.5 μm, 5.2 μm and 6 μm, respectively. The gradient of the width-distance curve is reduced as the observed position from the interface increases. The tendency of the gradient will be discussed quantitatively in a later section.

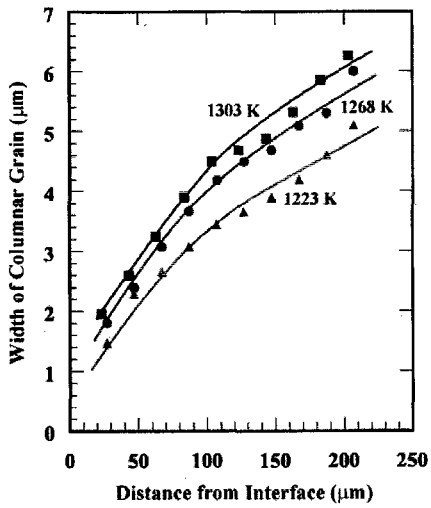

Fig.5 Mean width of columnar grains as a function of the distance from the coating/substrate interface.

3.3 Nucleation on the substrate

We can roughly estimate the spacing between initial nuclei on the substrates using extrapolation of the width-distance curves in Fig.5. When the gaps between the neighboring columns are neglected, the value of the mean width of the columnar grains at 0 μm must correspond to the spacing between initial nuclei. The values of sizes of nuclei are estimated to be 0.28 μm, 0.60 μm and 1.12 μm for samples produced at 1223 K, 1268 K and 1303 K, respectively. Therefore, the densities of nuclei were calculated to be 13.0 μm^{-2}, 2.8 μm^{-2} and 0.8 μm^{-2}.

An Arrhenius plot of the density of nuclei is shown in Fig.6. Since the relationship between the density of the nuclei and the reciprocal of the processing temperature is linear, it is suggested that the formation of nuclei obeys the Arrhenius equation. We should note that vapor flux increases as the processing temperature is raised under our deposition conditions as seen in Table I.

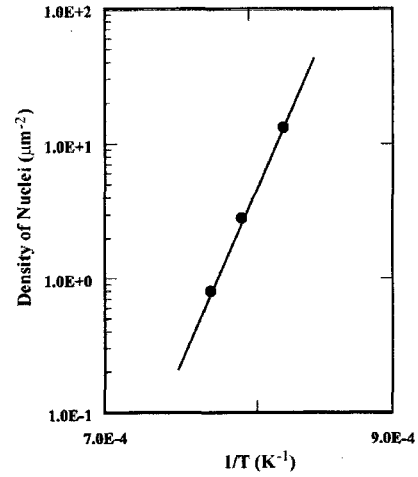

Fig.6 Arrhenius plot of density of nuclei on the substrate.

Therefore, from the viewpoint of vapor flux, the formation of nuclei easily occurs at higher processing temperatures. In contrast, the density of nuclei in the sample deposited at a lower temperature is higher. This result suggests that the influence of the degree of supercooling is stronger than that of the vapor flux. We can estimate the density of nuclei, n [μm^{-2}], as follows;

$$n = 2.48\times10^{-19}\exp\left(\frac{55562}{T}\right). \quad (1)$$

3.4 Kinetics of columnar grain growth

Many researchers have reported that competitive grain growth of crystals on a substrate can be expressed by the following equation;

$$w = Ah^n \quad (2)$$

where w is the crystal width; h is the distance from the

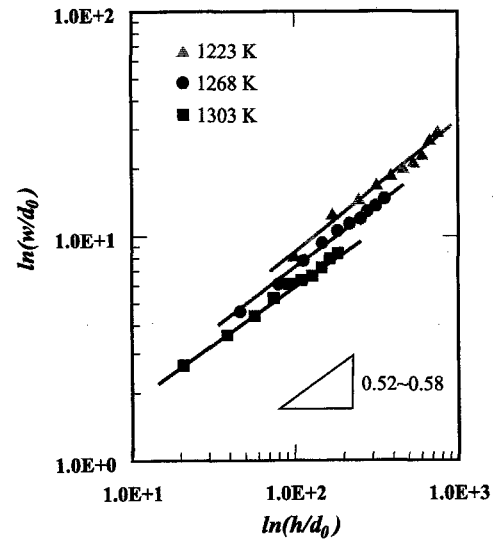

Fig.7 Relationship between the mean width of the columnar grains and the distance from the interface. These values are normalized to the size of nuclei at each temperature for comparison.

coating/substrate interface; and A and n are constants.

We replotted the data of the mean width of the columnar grains on a double logarithmic scale in Fig.7. The exponential constant, n, in Eq.(2) at each sample was estimated to vary from 0.52 to 0.58 from the figure. From theoretical considerations based on the "competitive crystal growth model", the exponent n was reported to be 0.4 ~ 0.5 [10-12]. Since our experimental values are close to the theoretical ones, the kinetics of columnar grain growth in EB-PVD TBCs can be explained using the competitive crystal growth model. The slight difference between the experimental and theoretical values probably results from the "shadowing effect" that is caused by blocking of vapor flux by neighboring columnar grains. Competition between the columnar grains will be enhanced by the shadowing effect. In addition, the constant A in Eq.(2) was evaluated to be 0.51 ~ 0.61.

The above-mentioned discussion suggests that the columnar structure formed under our processing conditions can be estimated by Eq.(1) and Eq.(2). However, in order to generalize these findings for columnar grain growth in EB-PVD TBCs, further experimental data of grain growth under various processing conditions will be required.

4. CONCLUSION

ZrO_2-4mol%Y_2O_3 TBC layers were produced on IN738LC substrates by the EB-PVD process. The processing temperatures were varied from 1223 K to 1303 K. While the crystal orientations of the layers are <100>, the coating textures changed depending on the processing temperatures. The mean width of the columnar grains in TBC layers increased as the processing temperatures were raised. Since the density of the initial nucleation on the substrate followed the Arrhenius equation, the degree of supercooling probably dominates the nucleation behavior in the EB-PVD process. Moreover, the kinetics of the evolution of the coating texture could be explained by an exponential law based on the competitive crystal growth model. These exponents were estimated to be 0.52~0.58 and the values were consistent with results reported from theoretical considerations.

ACKNOWLEDGEMENT

This work was performed as a part of the Nanostructure Coating Project supported by the New Energy and Industrial Technology Development Organization of Japan.

REFERENCES

[1] R. K. Matta, GER-3935B (2000).
[2] S. Aoki, ASME IJPGC2000-15084, 1-6 (2000).
[3] G. W. Goward, Surf. Coat. Technol., 108-109, 73-79 (1998).
[4] M. Peters, C. Leyens, U. Schulz and W. A. Kaysser, Advanced Engineering Materials, 3-4, 193-204 (2001).
[5] E. Lugscheider, C. Barimani and G. Döpper, Surf. Coat. Technol., 98, 1221-1227 (1998).
[6] U. Schulz, H. Oettel and W. Bunk, Z. Metallkd., 87-6, 488-492 (1996).
[7] S. G. Terry, J. R. Litty and C. G. Levi, Elevated Temperature Coating Science and Technology III, J. M. Hampikian and N. B. Dahotre (Eds), The Minerals, Metals & Materials Society, 13-25 (1999).
[8] D. D. Hass, P. A. Parrish and H. N. G. Wadley, J. Vac. Sci. Technol., A 16-6, 3396-3401 (1998).
[9] J. Shigh and D. E. Wolfe, J. Mater. Sci., 37, 3261-3267 (2002).
[10] A. N. Kolmogorov, Akad. Nauk SSSR, 65, 681 (1949).
[11] J. M. Thijissen, H. J. F. Knops and A. J. Dammers, Phys. Rev. B, 51, 1985 (1995).
[12] A. J. Dammers and S. Radelar, Proc. of the C90 Europhysics Conference on Computational Physics, A. Tenner (Eds), World Science (1991).

(Received October 10, 2003; Accepted March 31, 2004)